11

Formation Features of Stopbands in Bicomponent Magnetic Metasurfaces

© A.S. Bir[1], D.V. Romanenko[1], S.V. Grishin[1], S.A. Nikitov[1,2]

[1] Saratov National Research State University, Saratov, Russia
[2] Kotelnikov Institute of Radio Engineering and Electronics, Russian Academy of Sciences, Moscow, Russia
E-mail: sergrsh@yandex.ru

Received May 22, 2025
Revised August 11, 2025
Accepted August 30, 2025

The results of an experimental study and micromagnetic simulation of the formation features of the stopbands in bicomponent magnetic metasurfaces are presented. The metasurfaces consist of two magnetic materials: a dielectric film of yttrium iron grant (YIG) of micron thickness and a ferromagnetic metal (iron) film of nanometer thickness. From the iron film, a one-dimensional periodic structure in the form of submillimeter-sized stripes is formed on the free YIG film surface. It was found that in the spectrum of a magnetostatic surface spin wave (MSSW) propagating in the YIG film, there are the stopbands of three types. One of them are due to the reflection of the MSSW from the periodic structure (Bragg resonance), another by the resonance phenomena of spin waves inside the strips themselves, and the third by the MSSW resonances in the free YIG film region located between the input microstrip antenna and the closest (first) iron strip to it.

Keywords: metasurface, ferromagnetic, spin wave.

DOI: 10.61011/TPL.2026.01.62813.20381

Recently, magnonics research has seen an upsurge in interest in control of spin-wave transport in bicomponent (BC) two-dimensional (2D) periodic magnetic structures with period T being much smaller than wavelength λ ($T \ll \lambda$) [1–3]. Such artificially created magnetic structures are called magnetic metasurfaces [2]. These are planar (and, consequently, easier to fabricate) counterparts of three-dimensional metamaterials [4,5]. Magnonic crystals (one-dimensional (1D) and 2D periodic planar magnetic structures) with their period comparable to the wavelength ($T \sim \lambda$) [6] are now also regarded as magnetic metasurfaces. Their frequency-selective properties are of interest in the context of production of various filtering devices controlled by magnetic [7] or electric [8] fields, direct current [9–11], laser radiation [12], and even mechanical deformations [13], and their reconfigurable properties find use in logic circuits [14].

BC magnetic metasurfaces consist of two magnetic materials: either two metallic ferromagnets [15–20] or a metallic ferromagnet and a dielectric ferrimagnet [1–3]. One of the magnetic materials is used as a matrix, and the other magnetic material in the form of strips [3,15] or disks [1,2,16–20] forms a 1D or 2D periodic structure on its surface. If a metallic ferromagnet and a dielectric ferrimagnet are used simultaneously, the latter is an yttrium iron garnet (YIG) film from which a magnetic matrix is produced. A periodic structure is formed from a film of ferromagnetic metals (Ni [15], Co [16–19], Fe [20] or their compounds [1–3]) on the YIG matrix surface.

Experiments with BC magnetic metasurfaces were carried out using YIG matrices of both micrometer ($\sim 10^{-5}$ m) [3] and nanometer ($\sim (2-20) \cdot 10^{-8}$ m) [1,2] thickness. The authors of [3] have formed 1D and 2D periodic structures consisting of subwavelength elements, which had a rectangular/square shape and micrometer sizes and were fabricated based on a permalloy (Py) film, on the surface of a tangent-magnetized YIG matrix. It was demonstrated that the stopband in the spectrum of a traveling magnetostatic surface spin wave (MSSW) may be controlled by adjusting the orientation of an external constant magnetic field relative to the direction of MSSW propagation. The indicated stopband did not satisfy the Bragg condition ($k_B = n\pi/T$ — Bragg wave number that corresponds to frequency f_B; $n = 1, 2, 3\ldots$ — Bragg resonance number). If this condition is fulfilled, stopbands form in the MSSW spectrum due to MSSW reflection from the periodic structure. In [2], 2D periodic structures consisting of subwavelength elements, which had the shape of disks of submicrometer sizes and were fabricated based on $Co_{20}Fe_{60}B_{20}$, Co, and Py ($Ni_{80}Fe_{20}$) ferromagnetic metal films, were formed on the surface of a tangent-magnetized YIG matrix. The emergence of a stopband in the spectrum of a traveling MSSW in this context is attributable to the dynamic relation between the resonance of the vortex state in ferromagnetic nanodisks and the MSSW traveling in the ferrite matrix.

It was demonstrated in [21] that a single 1D ferromagnetic strip allows one to form a stopband that does not satisfy the Bragg condition. The stopband was located in the high-frequency region of the spectrum of an MSSW traveling in a YIG matrix of a submicrometer thickness with a strip of CoFeB or Py on its surface. The strip width varied from $27 \cdot 10^{-8}$ to $5 \cdot 10^{-5}$ m. The stopband here was the result of destructive interference of an MSSW incident on the YIG/CoFeB (or YIG/Py) bilayer with a spin wave

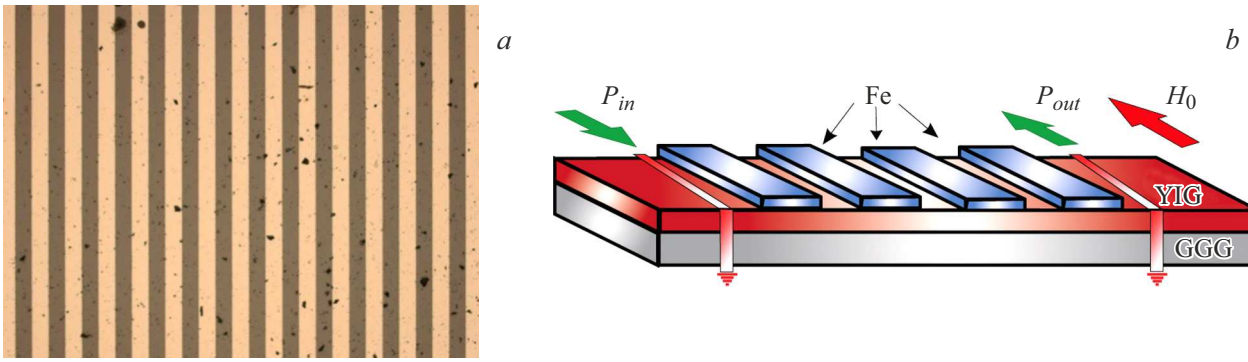

Figure 1. *a* — Photographic image of a fragment of a BC YIG/Fe magnetic metasurface with period $T = 16 \cdot 10^{-5}$ m obtained using an optical microscope. *b* — Schematic representation of a spin-wave transmission line based on a BC YIG/Fe magnetic metasurface with a 1D structure in the form of ferromagnetic strips. P_{in} — Input microstrip conductor power; P_{out} — output microstrip conductor power.

circulating inside the bilayer itself, which served as a Fabry–Pérot cavity.

In the present study, we use the example of BC metasurfaces made on the basis of a micrometer-thick YIG matrix with a 1D periodic structure of submillimeter-sized Fe strips deposited on its surface to demonstrate the feasibility of simultaneous formation of different stopbands, some of which are subject to the Bragg condition, while others are not subject to it.

BC magnetic metasurfaces fabricated based on a YIG film with thickness $d_1 = 12 \cdot 10^{-6}$ m and saturation magnetization $M_1 = 0.0139$ T, which were grown by liquid-phase epitaxy on a gadolinium-gallium garnet substrate with a thickness of $5 \cdot 10^{-4}$ m, were used in the experiment. A waveguide $15 \cdot 10^{-3}$ m in length and $4 \cdot 10^{-3}$ m in width was formed from the YIG film. One-dimensional periodic structures consisting of Fe strips with thickness $d_2 = 10^{-7}$ m, a width of $T/2$, and period $T = (16-96) \cdot 10^{-5}$ m were deposited on the surface of the YIG waveguide. These structures occupied an area of 6.5×4 mm and were fabricated using the methods of magnetron sputtering, wet etching, optical lithography, and lift-off photolithography. The manufacturing process utilized a multifunctional ultra-high vacuum magnetron deposition complex and a magnetron sputtering unit based on a VUP-5M vacuum setup. A fragment of one of the fabricated BC magnetic metasurfaces is shown in Fig. 1, *a*.

A microstrip transmission line model in the delay line configuration was used to excite and receive an MSSW propagating in the BC magnetic metasurface (Fig. 1, *b*). Microstrip conductors had a width of $3 \cdot 10^{-5}$ m and were positioned at a distance of $8 \cdot 10^{-3}$ m from each other. The YIG waveguide with the 1D periodic structure applied to its surface was positioned between the microstrip conductors. External constant magnetic field H_0 was applied parallel to the microstrip conductors and perpendicular to the direction of MSSW propagation.

Figure 2 shows the measured amplitude-frequency responses (AFRs) of the spin-wave transmission line based on the BC YIG/Fe magnetic metasurface with different periods and strip sizes of the 1D structure and the AFRs of the spin-wave transmission line based on the YIG waveguide without any 1D structure on its surface. It follows from the data presented in Fig. 2, *a* that the AFR of the spin-wave transmission line based on the BC metasurface with strips of the largest period ($T = 96 \cdot 10^{-5}$ m) and width ($T/2 = 48 \cdot 10^{-5}$ m) features well-pronounced stopbands. One of them (higher-frequency band) satisfies the Bragg condition and corresponds to the first Bragg resonance, while the other (lower- frequency one) does not satisfy the Bragg condition and is not observed in the AFR of the YIG waveguide without a periodic 1D structure on its surface. The depth of stopbands (the difference between the attenuation level at the stopband frequency and the attenuation level at the same frequency determined without a periodic structure) is 20 dB (for the lower-frequency band) and 24 dB (for the Bragg band); their 3 dB Q-factors measured relative to the attenuation level at the stopband frequency are equal to 657 and 836, respectively. In addition, the loss level rises significantly in the high-frequency region of the AFR of the transmission line based on the 1D metasurface, which leads to narrowing of the AFR compared to that of the transmission line based on a homogeneous YIG film.

Figure 2, *b* shows the AFR of the spin-wave transmission line with a BC metasurface with its structure period and strip width being 3 times smaller than the corresponding dimensions of the structure considered earlier. Only one (lower-frequency) stopband is seen in the AFR of this transmission line. Its central frequency does not satisfy the Bragg condition, and its position in the MSSW spectrum is virtually independent of the change in size of the periodic structure. The depth of the low-frequency stopband increases to 27.4 dB, and its Q-factor is 4306. The latter figure is quite sufficient for high-Q stop-band filters based on magnetostatic spin waves. At the same time, the frequency corresponding to the first Bragg resonance now lies outside the MSSW excitation band. In addition, the use of a periodic structure with smaller dimensions leads to a significant increase in losses in the high-frequency region of

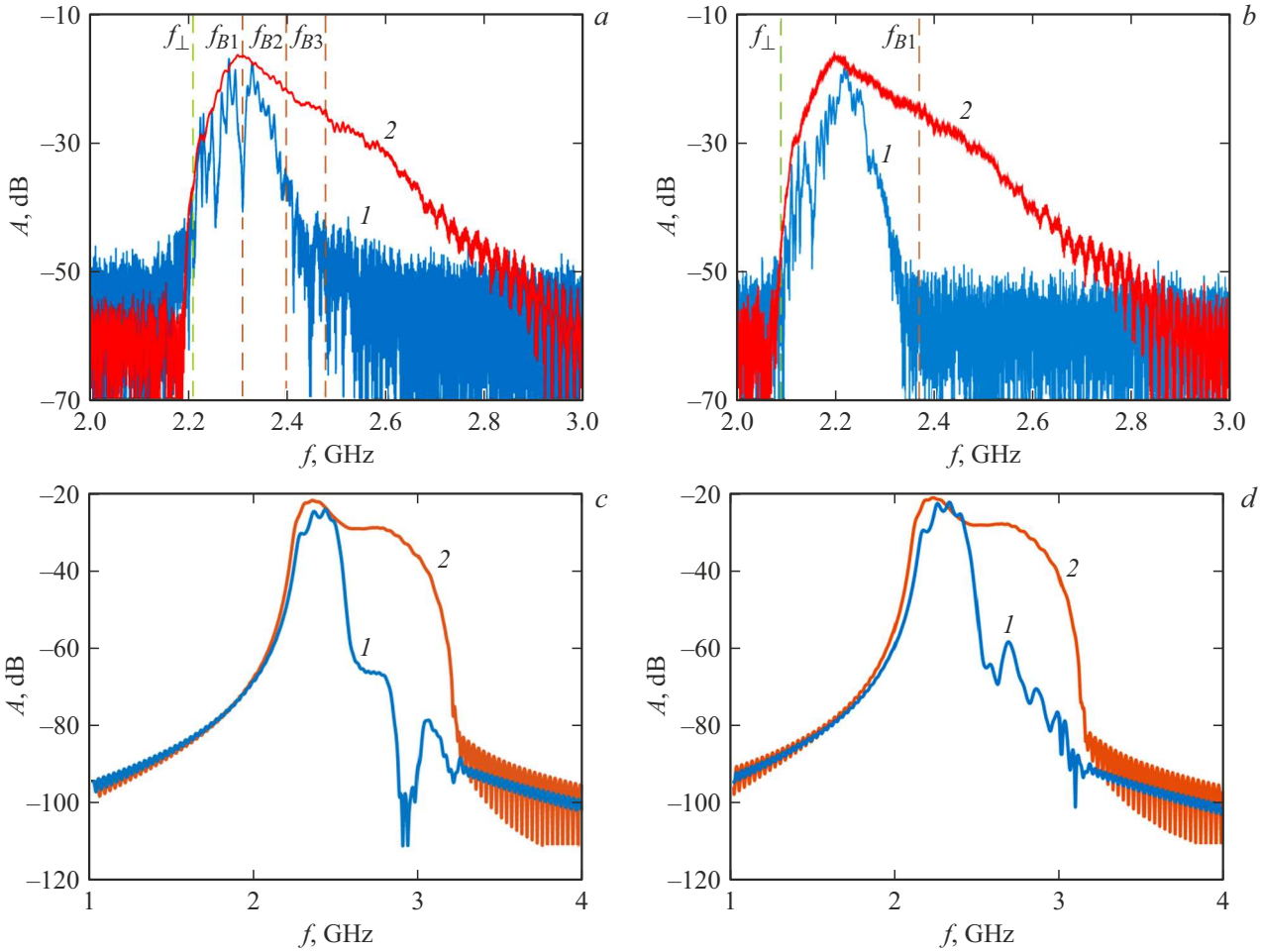

Figure 2. AFRs of a spin-wave transmission line with a BC YIG/Fe magnetic metasurface obtained in a radiophysical experiment (*a*, *b*) and calculated in the MuMax^3 software package (*c*, *d*). *a*, *b* — Results for a periodic structure with different periods T and widths W of Fe strips (curves *1*): $T = 96 \cdot 10^{-5}$ m, $W = 48 \cdot 10^{-5}$ m (*a*) and $T = 32 \cdot 10^{-5}$ m, $W = 16 \cdot 10^{-5}$ m (*b*). *c*, *d* — Results for a YIG film loaded with a single Fe strip (curves *1*) with its width W equal to $48 \cdot 10^{-5}$ (*c*) or $16 \cdot 10^{-5}$ m (*d*). Curves *2* in all panels correspond to the results obtained for a homogeneous YIG film. $H_0 = 24.11$ (*a*, *c*) and 21.88 kA/m (*b*, *d*).

the MSSW spectrum. Owing to this, the MSSW excitation band also becomes narrower than the one observed in the case where a 1D structure on the YIG film surface is lacking. A similar effect has been observed earlier in [3] where a 1D periodic structure of micrometer-wide Py strips was formed on the YIG film surface. However, in contrast to the results reported in [3], a well-pronounced stopband was also observed in the low-frequency region of the MSSW spectrum in our experiments when the periodic structure was not rotated relative to the direction of field H_0.

We believe that the emergence of a low-frequency stopband is associated with the formation of a standing MSSW in the region of the free YIG film that is located between the input microstrip antenna and the closest (first) iron strip. This region has a length of $\sim (0.5{-}1) \cdot 10^{-3}$ m, which varies between YIG waveguides with different periodic structures, and a MSSW with a similar wavelength resonates in it, reflecting alternately from the first iron strip and the input microstrip antenna. Specifically, the MSSW wavenumber at $H_0 = 24.11$ kA/m and $W = 48 \cdot 10^{-5}$ m (Fig. 2, *a*) is $\sim 14 \cdot 10^2$ m^{-1} at a resonant frequency of 2253 MHz of the low-frequency stopband; at $H_0 = 21.88$ kA/m and $W = 16 \cdot 10^{-5}$ m (Fig. 2, *b*), the MSSW wavenumber ($\sim 19 \cdot 10^2$ m^{-1}) corresponds to a resonant frequency of 2152 MHz. Thus, the weak dependence of the MSSW wavenumber corresponding to the central frequency of the stopband on period and width of iron strips and the vanishing of this stopband in a YIG film without a 1D structure support the above assumption.

Numerical modeling of the transfer characteristic of a YIG film with a thickness of $12 \cdot 10^{-6}$ m and a single Fe strip with a thickness of $2 \cdot 10^{-7}$ m, a varying width, and saturation magnetization $M_2 = 0.1751$ T positioned on its surface was performed in order to confirm the fact that the increase in losses in the high-frequency region of the MSSW spectrum is attributable in both cases to the resonant properties of magnetic strips. The results obtained in the MuMax^3 micromagnetic modeling software package are

shown in Figs. 2, *c*, *d*. It follows from the presented data that, as in the experiment, the AFRs of layered structures are more narrow-band in both cases than those calculated for a free YIG film. This is associated with the emergence of a relatively wide stopband, the depth of which decreases with decreasing width of the Fe strip, in the high-frequency region of the MSSW spectrum. However, the low-frequency stopband known from our experiments is not found in the numerical modeling data, which is attributable to the fact that MuMax[3] lacks the capacity to simulate a microstrip transmission line.

The obtained results are of interest for the design of filtering devices for magnonics and magnonic spintronics [22,23].

Funding

This study was supported by a grant from the Russian Science Foundation (project No. 19-79-20121).

Conflict of interest

The authors declare that they have no conflict of interest.

References

[1] S. Watanabe, V.S. Bhat, A. Mucchietto, E.N. Dayi, S. Shan, D. Grundler, Adv. Funct. Mater., **35** (31), 2301087 (2023). DOI: 10.1002/adma.202301087
[2] H. Yu, J. Chen, V. Cros, P. Bortolotti, H. Wang, C. Guo, F. Brandl, F. Heimbach, X. Han, A. Anane, D. Grundler, Adv. Funct. Mater., **32** (34), 2203466 (2022). DOI: 10.1002/adfm.202203466
[3] S.L. Vysotskii, Yu.V. Khivintsev, V.K. Sakharov, N.N. Novitskii, G.M. Dudko, A.I. Stognii, Yu.A. Filimonov, Phys. Solid State, **62** (9), 1659 (2020). DOI: 10.1134/S1063783420090334.
[4] S.B. Glybovski, S.A. Tretyakov, P.A. Belov, Yu.S. Kivshar, C.R. Simovski, Phys. Rep., **634**, 1 (2016). DOI: 10.1016/j.physrep.2016.04.004
[5] H.-T. Chen, A.J. Taylor, N. Yu, Rep. Prog. Phys., **79**, 076401 (2016). DOI: 10.1088/0034-4885/79/7/076401
[6] K. Zakeri, J. Phys.: Condens. Matter., **32** (36), 363001 (2020). DOI: 10.1088/1361-648X/ab88f2
[7] A.S. Bir, S.V. Grishin, D.V. Romanenko, S.A. Nikitov, IEEE Trans. Magn., **60** (9), 2800205 (2024). DOI: 10.1109/TMAG.2024.3425901
[8] M.A. Morozova, D.V. Romanenko, A.A. Serdobintsev, O.V. Matveev, Yu.P. Sharaevskii, S.A. Nikitov, J. Magn. Magn. Mater., **514** (15), 167202 (2020). DOI: 10.1016/j.jmmm.2020.167202
[9] A.V. Chumak, T. Neumann, A.A. Serga, B. Hillebrands, M.P. Kostylev, J. Phys. D, **42** (20), 205005 (2009). DOI: 10.1088/0022-3727/42/20/205005
[10] A.A. Nikitin, A.B. Ustinov, A.A. Semenov, A.V. Chumak, A.A. Serga, V.I. Vasyuchka, E. Lähderanta, B.A. Kalinikos, Appl. Phys. Lett., **106** (10), 102405 (2015). DOI: 10.1063/1.4914506
[11] A.S. Bir, S.V. Grishin, A.A. Grachev, O.I. Moskalenko, A.N. Pavlov, D.V. Romanenko, V.N. Skorokhodov, S.A. Nikitov, Phys. Rev. Appl., **21** (4), 044008 (2024). DOI: 10.1103/PhysRevApplied.21.044008
[12] A.S. Bir, M.A. Morozova, D.V. Romanenko, S.A. Nikitov, S.V. Grishin, Tech. Phys. Lett., **49** (11), 63 (2023). DOI: 10.61011/TPL.2023.11.57203.19701.
[13] A.V. Sadovnikov, A.A. Grachev, A.A. Serdobintsev, S.E. Sheshukova, S.S. Yankin, S.A. Nikitov, IEEE Magn. Lett., **10**, 5506405 (2019). DOI: 10.1109/LMAG.2019.2943117
[14] A. Khitun, M. Bao, K.L. Wang, J. Phys. D, **43**, 264005 (2010). DOI: 10.1088/0022-3727/43/26/264005
[15] M. Mruczkiewicz, P. Graczyk, P. Lupo, A. Adeyeye, G. Gubbiotti, M. Krawczyk, Phys. Rev. B, **96** (10), 104411 (2017). DOI: 10.1103/PhysRevB.96.104411
[16] P. Malagò, L. Giovannini, R. Zivieri, P. Gruszecki, M. Krawczyk, Phys. Rev. B, **92** (6), 064416 (2015). DOI: 10.1103/PhysRevB.92.064416
[17] M. Krawczyk, S. Mamica, M. Mruczkiewicz, J.W. Klos, S. Tacchi, M. Madami, G. Gubbiotti, G. Duerr, D. Grundler, J. Phys. D, **46** (49), 495003 (2013). DOI: 10.1088/0022-3727/46/49/495003
[18] S. Tacchi, G. Duerr, J.W. Klos, M. Madami, S. Neusser, G. Gubbiotti, G. Carlotti, M. Krawczyk, D. Grundler, Phys. Rev. Lett., **109** (13), 137202 (2012). DOI: 10.1103/PhysRevLett.109.137202
[19] G. Duerr, M. Madami, S. Neusser, S. Tacchi, G. Gubbiotti, G. Carlotti, D. Grundler, Appl. Phys. Lett., **99** (20), 202502 (2011). DOI: 10.1063/1.3662841
[20] F.S. Ma, H.S. Lim, Z.K. Wang, S.N. Piramanayagam, S.C. Ng, M.H. Kuok, Appl. Phys. Lett., **98** (15), 153107 (2011). DOI: 10.1063/1.3579531
[21] H. Qin, R.B. Holländer, L. Flajšman, F. Hermann, R. Dreyer, G. Woltersdorf, S. van Dijken, Nat. Commun., **12**, 2293 (2021). DOI: 10.1038/s41467-021-22520-6
[22] S.A. Nikitov, A.R. Safin, D.V. Kalyabin, A.V. Sadovnikov, E.N. Beginin, M.V. Logunov, M.A. Morozova, S.A. Odintsov, S.A. Osokin, A.Yu. Sharaevskaya, Yu.P. Sharaevsky, A.I. Kirilyuk, Phys. Usp., **63** (10), 945 (2020). DOI: 10.3367/UFNe.2019.07.038609.
[23] A.V. Chumak, V.I. Vasyuchka, A.A. Serga, B. Hillebrands, Nat. Phys., **11**, 453 (2015). DOI: 10.1038/nphys3347

Translated by D.Safin